Recent Trend of Multiuser MIMO in LTE-Advanced

Chaiman Lim, Korea University

Taesang Yoo, Qualcomm Incorporated

Bruno Clerckx, Imperial College, London

Byungju Lee and Byonghyo Shim, Korea University

Abstract

Recently, the mobile communication industry is moving rapidly towards long-term evolution (LTE) systems. The leading carriers and vendors are committed to launching LTE service in the near future and, in fact, number of major operators such as Verizon has initiated LTE service already. LTE aims to provide improved service quality over 3G systems in terms of throughput, spectral efficiency, latency, and peak data rate, and MIMO technique is one of the key enablers of the LTE system for achieving these diverse goals. Among several operational modes of MIMO, multiuser MIMO (MU-MIMO), in which the base station transmits multiple streams to multiple users has received much attention as a way for achieving improvement in performance. From the initial release (Rel. 8) to the recent release (Rel. 10) so called LTE-Advanced, MU-MIMO techniques have been evolved from its premature form to the more elaborated version. In this article, we provide an overview of design challenges and the specific solutions for MU-MIMO systems developed in LTE-Advanced standard.

Recent Trend of Multiuser MIMO in LTE-Advanced

I. Introduction

Recent explosion of smart-phone users and ever-increasing demand for high quality multimedia over wireless are fueling the deployment of long term evolution (LTE) mobile communication systems [1], [2]. Initiated in 2004, the LTE standardization effort focuses on enhancing the Universal Terrestrial Radio Access (UTRA) and optimizing the 3GPP's radio access architecture. Initial design targets of the LTE were to have the average user throughput of about three times that of the release 6 HSDPA's in the downlink (100Mbps) and about three times that of the HSUPA's in the uplink (50Mbps). Its initial release (Rel. 8), which has been the basis for the LTE standard, was finalized in Dec. 2008, and a subsequent release (Rel. 9) was frozen in Dec. 2009. Standardization of the latest release (Rel. 10), popularly called LTE-Advanced (LTE-A), has been closed in Jun. 2011 and LTE Rel-11 is currently under development.

Among many features in the LTE-A which supports up to 3Gbps throughput in downlink, multiuser multiple-input-multiple-output (MU-MIMO) scheme has been identified as one of the key enablers for achieving a high spectral efficiency [3]. Both in theory and design perspectives, MU-MIMO systems have several unique features distinct from single user MIMO (SU-MIMO) systems. Although both systems provide spatial multiplexing gains that are effective in improving the throughput, cell coverage, and reliability of mobile communication systems, the SU-MIMO systems are vulnerable in scenarios where the spatial multiplexing capability of a single user's channel is limited either due to SINR (signal to interference and noise ratio) or fading correlations among antenna elements or by the number of receive antennas at the user side. To make up for the shortcomings of SU-MIMO, early LTE standards (Rel. 8 and 9) defined a primitive form of the MU-MIMO mode. The operations of MU-MIMO are elaborated and enhanced in the LTE-A standard (Rel. 10). Our purpose in this article is to provide an overview of the key features of MU-MIMO systems defined/adopted in the LTE and LTE-A standards.

Key distinctions between MU-MIMO and SU-MIMO systems

Information theory highlights some key aspects of MU-MIMO systems over SU-MIMO systems. Firstly, it is well known that when the channel matrix is full rank, the capacity gain of SU-MIMO systems is scaled by $\min\{M, N\}$ at high SNR, where M and N are the number of antennas at the transmitter and the receiver, respectively. In typical cellular systems, the number of receive antennas at the battery powered user (user equipment; UE) is often smaller than the number of transmit antennas at the base station (enhanced node-B; eNB), limiting the gain of SU-MIMO systems to the number of antennas at the receiver. In contrast, under the assumption that the transmitter has perfect CSIT (channel state information at the transmitter), the sum capacity of MU-MIMO is scaled by $\min\{M, Nn\}$, where n is the number of users multiplexed into the MU-MIMO transmission, so that M-fold increase in the sum rate can be obtained as long as Nn is larger than M.

Secondly, it has been shown that SU-MIMO systems are susceptible to the ill-behavior of propagation channels such as a strong line of sight (LOS) path or strong correlations among antenna elements. In such cases, the effective rank of the channel matrix decreases and so does the capacity gain of SU-MIMO. On the other hand, with the additional degrees of freedom introduced by the co-scheduling of multiple UEs, MU-MIMO systems can be designed less sensitive to the ill behavior of the channel matrix, allowing MU-MIMO systems to achieve the full multiplexing gain regardless of the effective rank of each individual user.

Challenges of MU-MIMO systems

In theoretical perspective, one of the major benefits of MU-MIMO systems is the realization of the full spatial multiplexing gain. Supporting MU-MIMO operations, however, requires appropriate resource allocation, in particular, among users. The aim of the user allocation is to choose a group of UEs that, when co-scheduled, maximizes a predefined performance metric (such as the sum throughput). To achieve this objective, channel state information (CSI) of UEs should be fed back to the eNB. A practical problem related to the CSI feedback is the balancing of the feedback accuracy and the uplink resource consumption caused by the feedback. Since feeding back real numbered CSI would require an infinite number of bits, the CSI needs to be represented, e.g. via appropriate quantization, with a limited number of bits. Note that while the accuracy of the CSI affects the SNR offset but not the multiplexing gain in SU-MIMO systems, such is not the case for MU-MIMO systems. In fact, since MU-MIMO systems are interference

TABLE I

THE NOMENCLATURE OF MU-MIMO RELATED TERMINOLOGIES IN LTE STANDARD

LTE standard	**MU-MIMO terminology**
Reference Signal (RS)	Pilot signal
User Equipment (UE)	User terminal, Mobile
Enhanced NodeB (eNB)	Base station
Precoding matrix indicator (PMI)	Precoding codebook index
Rank indication (RI)	MIMO channel rank
Physical Downlink Shared Channel (PDSCH)	Downlink data channel
Physical Downlink Control Channel (PDCCH)	Downlink control channel

limited under the finite-rate feedback constraint, the level of feedback accuracy directly affects the multiplexing gain of the MU-MIMO downlink [4]. Another important problem related to the CSI feedback is how to determine channel quality information (CQI) to be fed back. Unlike SU-MIMO systems, a UE in MU-MIMO cannot accurately estimate its SINR, due to the lack of knowledge of eNB's beam selections for co-scheduled UEs. Such knowledge is typically unavailable to the UE at the time of CQI calculation, as it is a function of the eNB's scheduling decision that will in turn be dependent on the UEs' CSI feedback.

In the rest of this article, we provide an overview of MU-MIMO techniques adopted in LTE and LTE-A. In particular, Section II summarizes features of MU-MIMO and rationale behind them defined in Rel. 8/9 LTE. Section III is devoted to MU-MIMO techniques adopted in LTE-Advanced as well as the technical grounds behind each decision. Finally, Section IV concludes the paper. Since terminologies of LTE standards might be unfamiliar to the reader, we put a summary of commonly used technical terms and their mappings to LTE standards in Table I.

II. MU-MIMO IN RELEASE 8/9 LTE

LTE Rel. 8 supports a primitive form of the MU-MIMO as a direct extension of its SU-MIMO closed-loop spatial multiplexing mode. In a nutshell, the MU-MIMO in Rel. 8 LTE employs a codebook based precoding, wherein each UE measures its spatial channel using the common RS (CRS) broadcasted from the eNB, selects the rank-1 precoder that best represents the channel from a predefined codebook set, and then feeds back the index (PMI) of the codebook as well as

the resulting CQI to the eNB via an uplink channel. The eNB collects the PMI and CQI reports from different UEs and performs user grouping onto the given time/frequency resource such that the paired UEs experience minimum level of inter-stream interference among themselves. It is important to note that, as far as the feedback is concerned, the UE does not differentiate the MU-MIMO from the SU-MIMO. That is, the CQI at the UE is computed based on the assumption that there is no inter-stream interference caused by the concurrent transmission from the eNB to a co-scheduled user. Since the CQI generated in this way would be a bit optimistic, the eNB may need to apply a back-off to the reported CQI to choose a right modulation order and code rate for the UE. On top of this, an additional 3dB backoff is required as the power needs to be shared by the two UEs.

Rel. 8 MU-MIMO (a.k.a transmission mode 5) does not define a dedicated pilot. Hence, the UE should rely on the CRS for channel estimation and demodulation of data. As the CRS is un-precoded, the UE should explicitly derive the precoded channel by multiplying the estimated channel with the precoding information separately signaled to the UE through a control channel. A drawback of this approach is that the eNB's choice of precoding matrix is confined to those defined in the codebook.[1] This limitation is relaxed in Rel. 10 as will be discussed in the next section.

Rel. 8 MU-MIMO relies on a single wideband PMI reporting per UE, representing the average channel direction over the entire system bandwidth. Such a lack of frequency-selective PMI reporting essentially limits the usefulness of MU-MIMO to cells with a highly correlated uniform linear array (ULA) antenna configuration, in which UEs typically experience rank-1 channels with rather non-frequency-selective eigenbeam directions.

Also, in Rel. 8, the SU-MIMO and MU-MIMO modes are semi-statically switched. Although a dynamic switching between two modes may in principle allow more flexibility in the scheduling and increase multiuser diversity, the lack of MU-MIMO-specific CQI reporting and the limited precoding mechanism in Rel. 8 diminish the benefit of the dynamic switching. In fact, Rel. 8 MU-MIMO is seen beneficial only in certain scenarios, i.e. for heavily loaded cells with

[1]In general, it may be beneficial for the eNB to choose a precoding matrix outside of the pre-defined codebook, an approach also known as the non-codebook precoding. For example, the eNB may want to use zero-forcing beams computed by inverting the composite channel matrix constructed by stacking the rank-1 channel vectors corresponding to PMIs.

highly correlated ULA antennas. Considering these factors and also design simplicity, semi-static switching was chosen in Rel. 8.

In addition to CRS-based transmissions, Rel. 9 supports rank-2 transmissions (called dual layer beamforming) using the demodulation RS (DM-RS). Unlike the CRS which is common to all users in a cell and hence cannot be precoded, the DM-RS is UE-specific, i.e. dedicated to each UE and precoded along with accompanying data. Note that when the pilot is precoded, the precoder information does not need to be separately delivered to the UE. In this sense, the use of precoded DM-RS makes the operation of the eNB *transparent* to the UE and enables the use of non-codebook based precoding. In the dual layer beamforming, an orthogonal cover code (OCC) of length two is used to differentiate pilots on two layers. In addition, by defining two scrambling IDs, the Rel-9 dual layer beamforming can support up to 4 stream multiplexing, wherein the two groups are differentiated by distinct scrambling IDs, and the two layers within each group are separated by an OCC. This allows the eNB to schedule two UEs simultaneously in a MU-MIMO mode, with two layers assigned for each UE.[2]

III. Multiuser MIMO in LTE-Advanced

A. Brief Overview

LTE-A systems should meet various requirements of ITU-R including peak, average, cell edge spectrum efficiencies [5]. Several new features have been introduced in Rel. 10 to achieve these goals. First, in order to support a high dimensional SU-MIMO operation (up to 8×8 MIMO) and also to improve the MU-MIMO operation, new RSs have been introduced in the downlink. There are three different kinds of RSs – CRS, DM-RS, and CSI (channel state information)-RS. The CRS is used for CSI measurements and demodulation in legacy (Rel. 8 and 9) transmission modes, as well as for control channel decoding and various measurements and UE procedures. The DM-RS, introduced in Rel. 9, is extended in Rel. 10 to support up to rank 8 transmissions in new transmission modes. The CSI-RS, newly introduced in Rel. 10, is used for CSI measurements in the new transmission modes. Second, dynamic switching between SU-MIMO and MU-MIMO is adopted. With the use of DM-RS, eNB can flexibly switch the MIMO operation mode of the UEs with no need to inform the precoding information to the UEs. This helps the eNB to

[2]However, the DM-RS between two groups is only quasi-orthogonal.

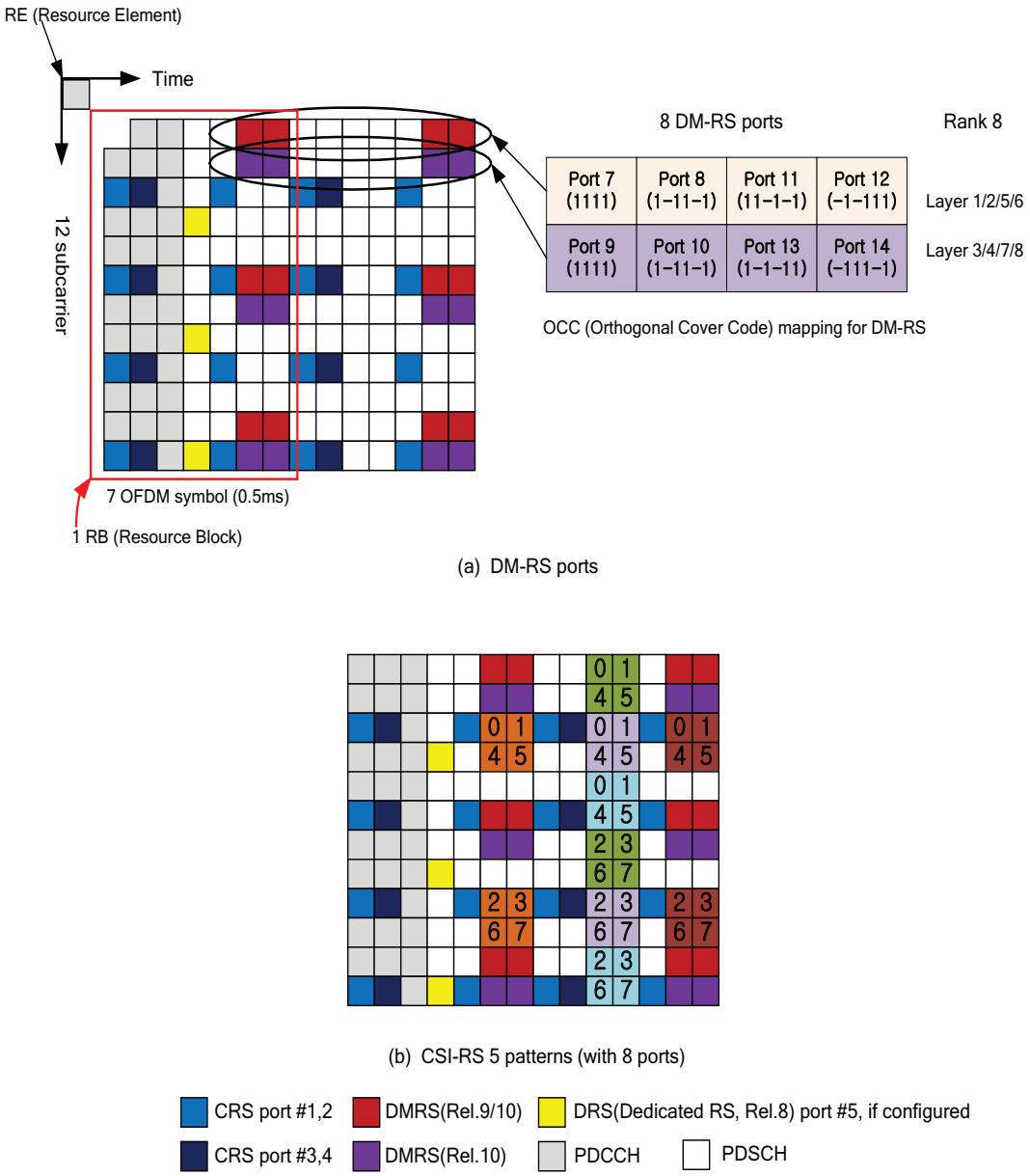

Fig. 1. DM-RS and CSI-RS patterns.

promptly respond to the variations in the channel and system conditions such as the traffic type and the number of UEs. Third, as an effort to reduce feedback load, a dual codebook structure is adopted for the 8Tx configuration, where one codebook targets capturing wideband and long term channel properties, while the other is designed to capture frequency-selective and/or short term channel properties.

B. Reference Signal Design

Over the past years, practical schemes achieving a fair amount of the capacity yet requiring reasonable precoding cost have been suggested [6], [7]. It is widely known that the gain of these techniques over a unitary precoding is considerable. This gain, however, is guaranteed only when the accuracy of the CSI feedback is high enough. To maintain a reasonable CSI estimation quality while avoiding the excessive pilot overhead, instead of a simple extension of CRS, Rel. 10 has adopted a separate DM-RS/CSI-RS approach. Main features of the reference scheme in Rel. 10 are as follows:

- CRS is defined for only up to 4 transmit antennas to limit the pilot overhead.
- In the new transmission mode of Rel. 10 (transmission mode 9; TM 9), the DM-RS is used for data demodulation of up to rank 8.
- In the TM 9, CSI measurements are performed using the CSI-RS. The CSI-RS is defined for up to 8 transmit antennas but with much lower overhead compared to the CRS.
- In legacy transmission modes which can support up to rank 4, channel estimation and CSI measurements are performed using the CRS.

Note that the DM-RS is not appropriate for CSI measurements as the DM-RS is precoded in a UE-specific manner. That is, the DM-RS is present only on time/frequency resources where the UE is scheduled data. CSI-RS, on the other hand, is unprecoded and defined over the entire system bandwidth for the CSI measurement. In order to minimize overhead, CSI-RS is transmitted in a fraction of subframes (see Fig. 1). This is in contrast to the CRS, which is used for both demodulation and CSI measurements and therefore needs to be transmitted every subframe.

Unlike CRS, the DM-RS needs to be transmitted only for the active spatial layers where data is present. Thus, the DM-RS is advantageous in terms of the pilot overhead if the rank of the data transmission is less than the number of transmit antennas, which is typically the case in 8 Tx antenna deployments. In fact, the DM-RS patterns in Rel. 10 are optimized for each rank to minimize the pilot overhead. The DM-RS patterns for ranks 3-8 in Rel. 10 are natural extensions of that for rank 2 in Rel. 9 and are based on a hybrid code/frequency division multiplexing; for ranks 1 and 2, the DM-RS patterns for the 1st and 2nd layers are multiplexed by code division multiplexing (CDM), while for ranks 3 and 4, DM-RS patterns for the 1st and 2nd layers and

for the 3rd and 4th layers are multiplexed by frequency division multiplexing (FDM). Hybrid CDM+FDM DM-RS patterns are adopted for ranks 5-8 with 2 CDM groups.

C. MU-MIMO Dimensioning

Considering the tradeoff between performance and signaling overhead, Rel. 10 has made the following decisions on the dimensioning of MU-MIMO systems:

- No more than 4 UEs are co-scheduled.
- No more than 2 layers are allocated per UE.
- No more than 4 layers are transmitted in total.

Multiplexing 4 UEs implies that each UE receives only a quarter of the total transmit power and that the UEs are also subject to substantial inter-user interference. Allocation of 4 UEs would be viable in a situation where the cell contains a large number of UEs with high SNRs and the rate gain due to the spatial multiplexing and multiuser diversity outweighs the per-UE rate loss caused by the power splitting and increased interference. Since scheduling more than 4 UEs in MU-MIMO results in overly complicated scheduling and UE implementation, and further such a scenario is uncommon in real deployments, this case will be rare in practice.

For example, four layers may be able to be supported in single-pole ULA systems, where spatial separation between UEs is easier. However, in a realistic deployment with dual-polarized arrays, it is very hard to control the MU-MIMO interference at the eNB with the feedback mechanism defined in Rel. 10. Hence, for systems with dual-polarized arrays, the number of co-scheduled users will be two for most cases.

With a highly correlated ULA, the eNB may direct 2 streams separately to 2 UEs and thereby obtain the spatial multiplexing benefits. This is particularly true in a highly loaded scenario where the increase in the spatial degrees of freedom can be achieved by a multi-user scheduling. Hence, a rank-1 transmission per UE may be the most common scenario for this case. The gain of having more than rank 1 is negligible in ULA but beneficial in dual-polarized systems. For example, in dual-polarized 8 Tx deployments, each polarization array can form a beam and direct a data stream to a UE, resulting in a rank-2 transmission per user.

D. Transparancy of MU-MIMO

In the transparent MU-MIMO mode, the UE can perform decoding with only its own control signal information (e.g., its own rank and DM-RS port). Whereas, information on co-scheduled UEs needs to be provided in the non-transparent MU-MIMO mode. The co-scheduling information includes the total rank and the DM-RS ports of co-scheduled UEs. Key distinctions between two modes and their implications on the system design are as follows:

- **Scheduling flexibility:** The transparent MU-MIMO allows for more flexible scheduling. For example, under the transparent MU-MIMO, resources (RBs) allocated for UEs multiplexed in MU-MIMO do not need to be fully aligned; the eNB may allocate partially overlapping resources to the UEs and may even multiplex different number of users on different RBs. Also, DM-RS ports of co-scheduled UE can be determined more dynamically for each RB. On the other hand, under the non-transparent MU-MIMO, the eNB may have to align resource allocations of co-scheduled UEs so that a single signaling of the total rank and the DM-RS ports of co-scheduled UEs is possible. This limits the scheduler flexibility and may compromise the performance of MU-MIMO systems.
- **Control-signaling overhead:** While transparent MU-MIMO requires no additional control signaling regarding co-scheduled UEs, non-transparent MU-MIMO requires more PDCCH resources to support user multiplexing and an advanced receiver operation of the UE. In transparent MU-MIMO, UE may have to resort to blind detection techniques to use advanced receiver algorithms. Also, UE complexity might be substantial to support functions such as modulation classification and enhanced channel estimation. Whereas, if its own DM-RS ports and co-scheduled DM-RS ports are delivered to the UE, channel information for the desired layers and the interfering layers can easily be estimated by the orthogonal DM-RS ports, and thereby an advanced receiver technique (e.g., interference rejection combining or non-linear interference cancellation) can be employed. In summary, for maximizing performance using the advanced receiver, information about DM-RS ports, number of co-scheduled UEs, MCS (modulation coding scheme) and rank of each UE are recommended in the downlink control signalings. Considering the limited budget for PDCCH, the increase in control information overhead is undesirable and may put a more stringent limit on the number of co-scheduled UEs per subframe. To address this issue, Rel. 11 is discussing

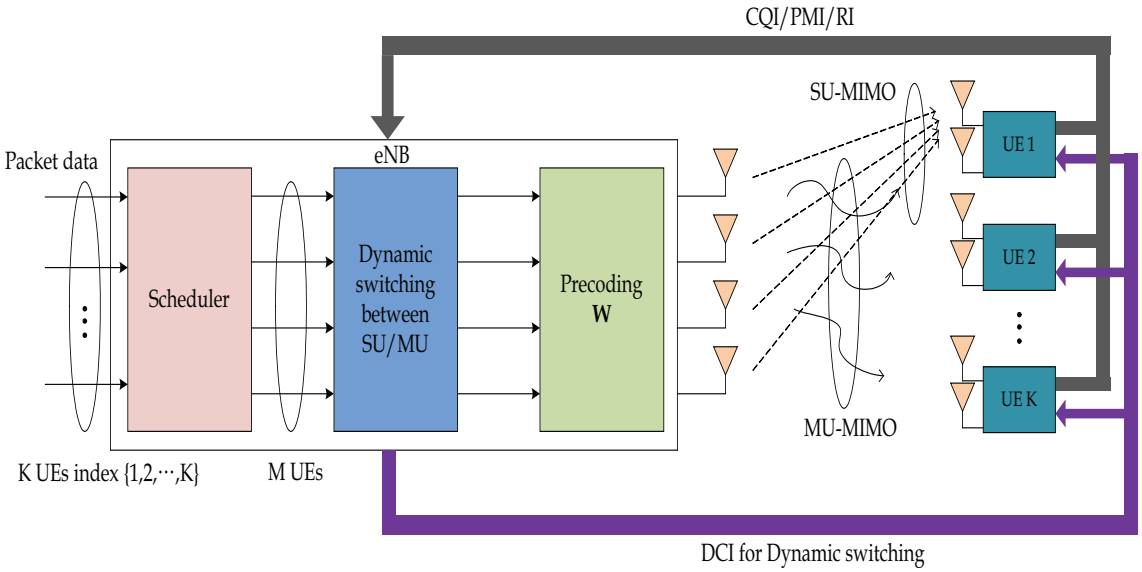

Fig. 2. SU/MU-MIMO Dynamic Switching

enhanced PDCCH on PDSCH region.

After weighing these pros and cons, Rel. 10 has decided to support transparent MU-MIMO. Additional signalling issues will be discussed in the upcoming releases.

E. SU/MU-MIMO Dynamic Switching

While SU-MIMO systems improve the peak/average UE throughput by transmitting multiple streams in the same time/frequency band, MU-MIMO systems provide a higher peak/average system throughput by exploiting multiuser diversity. To get the maximal benefit of both, Rel. 10 introduced a dynamic switching between the SU-MIMO and MU-MIMO modes (see Fig. 2). The main feature of the dynamic switching is to change the mode per subframe basis, based on the channel condition and traffic.

In order to support the SU/MU-MIMO dynamic switching, as well as the rank adaptation in the SU-MIMO mode, information on DM-RS antenna ports and the number of layers should be delivered to the UE. For this purpose, a new DCI (downlink control information) format, i.e. DCI format 2C, has been defined. As shown in Table II, the DCI format 2C contains antenna port information, the scrambling identity (SCID) of the DM-RS, and the number of layers. In LTE-A, the eNB can transmit up to 2 codewords by spatially multiplexing them into up to 8

TABLE II

ANTENNA PORT(S), SCRAMBLING IDENTITY AND NUMBER OF LAYERS INDICATION

One Codeword: Codeword 0 enabled, Codeword 1 disabled		Two Codewords: Codeword 0 enabled, Codeword 1 enabled	
	Message		Message
0	**1 layer, port 7, SCID=0**	0	**2 layers, ports 7-8, SCID=0**
1	**1 layer, port 7, SCID=1**	1	**2 layers, ports 7-8, SCID=1**
2	**1 layer, port 8, SCID=0**	2	3 layers, ports 7-9
3	**1 layer, port 8, SCID=1**	3	4 layers, ports 7-10
4	2 layers, ports 7-8	4	5 layers, ports 7-11
5	3 layers, ports 7-9	5	6 layers, ports 7-12
6	4 layers, ports 7-10	6	7 layers, ports 7-13
7	Reserved	7	8 layers, ports 7-14

layers. The bold faced entries in the table indicate message formats for the MU-MIMO and the rest indicate those for the SU-MIMO. The UE dimensioning and layer separation of Rel. 10 MU-MIMO is the same as that of Rel. 9 MU-MIMO discussed in the previous section.

F. CSI Feedback Mechanism

There are a number of factors that have been or will have to be considered in the design of the feedback mechanism in Rel. 10 and future releases. First of all, backward compatibility should be guaranteed; a Rel. 10 UE moving into a Rel. 8/9 network should be able to be configured to report feedback information (PMI, RI, and CQI) according to the Rel. 8/9 format for a seamless service. Likewise, PMI, RI, and CQI feedback mechanisms need to be supported for a Rel. 8/9 UE in the Rel. 10 network.

Second, feedback overhead should be investigated carefully. Overall, there exist two types of feedback mechanisms – explicit feedback and implicit feedback. Explicit feedback refers to the delivery of the channel matrix $\mathbf{H}$ and/or covariance matrix $\mathbf{H}^H\mathbf{H}$ from the UE to the eNB, while implicit feedback indicates the mechanism of the Rel. 8 feedback employing PMI, RI, and CQI. Considering its low feedback overhead, implicit feedback has been selected in Rel.

10. Nonetheless, since explicit feedback provides better scheduling flexibility, this issue will continue to be discussed in the future LTE-A releases.

Third, the UE feedback design should take real deployment scenarios into account. Note that device space limitations do not allow a large spacing at the eNB, not to mention at the UE. One commonly used technique for reducing the physical space is to employ dual-polarized antennas, where the antennas are grouped into pairs to form polarized collocated antennas.

In the standardization process, many approaches to improve the Rel. 8 implicit CSI feedback mechanism have been proposed [8]. We briefly describe key features of these schemes.

- **Adaptive codebook:** eNB can apply the transformed adaptive codebook on top of the fixed baseline codebook. UE may feedback an estimate of the correlation matrix or eigenvector to the eNB on long term basis. Any codebook may be used as the baseline codebook so that the Rel. 8 codebook could also be reused for this approach.
- **Differential feedback:** The differential feedback enables the eNB to track channel variation between adjacent feedbacks efficiently. Initially, the UE feeds back a full CSI as a reference. Next, the UE feeds back the difference between the previous CSI and the current one. The UE quantizes this difference using a differential codebook so that the index of the differential codebook is reported to eNB. Well-known drawback of the differential feedback is the sensitivity to the error propagation. Due to channel correlation between two adjacent channel blocks, the difference can be delivered with improved accuracy or lower overhead.
- **Multiple description coding (MDC):** In every PMI report, more than one PMI generated from different codebooks is provided to give different observation of the channel. By interpolating different observations, more accurate estimate of the channel can be obtained. While the differential codebook exploits temporal correlation between adjacent CSIs, such is not the case for the MDC since the collection of the PMI from distinct codebooks is used. Therefore, even if one PMI is dropped, the eNB can still estimate the channel by using the rest.
- **Best/Worst companion PMI:** This approach performs an additional feedback for better co-scheduling. Towards this end, both best and worst PMIs are delivered. Moreover, best companion report includes a delta CQI representing the SNR loss induced by the addition of another user on the same resource. Although additional overhead is relatively small, it is still non-negligible and the load of the scheduler to find the best UE pairs is considerable.

- **Multi-rank PMI/CQI:** This method reports multiple PMI/CQI pairs with different ranks. Each feedback corresponds to SU-MIMO with any rank or MU-MIMO with low rank. This multiple feedback information expedite dynamic switching between SU-MIMO and MU-MIMO.

G. Dual Codebook Operation

Rel. 10 adopted the multi-granular feedback structure referred to as the dual-stage feedback [8]. The precoder in the dual-stage feedback consists of two matrices ($\mathbf{W}_1$ and $\mathbf{W}_2$) and each of them is belonging to a separate codebook. A composite precoder is the product of the two and given by [9]

$$\mathbf{W} = \mathbf{W}_1\mathbf{W}_2, \tag{1}$$

where $\mathbf{W}_1$ is in charge of wideband and long term channel properties, and $\mathbf{W}_2$ captures frequency-selectivity and short term channel fading. A major advantage of decoupling the long-term and short-term CSI feedback components is a low feedback overhead and improved performance over the single codebook [10]. Below we provide major principles behind the Rel. 10 codebook design. The readers are referred to [11] for more details.

- The codebook design puts more emphasis on lower ranks (ranks 1 and 2), where the precoding gain is more pronounced.
- All entries in a precoding matrix need to have the same magnitude (constant modulus) to relieve the burden on the power amplifier design.
- Unitary precoding is preferred to maintain a constant average transmitted power.
- $\mathbf{W}_1(= [\mathbf{X}\ \ \mathbf{0}\,;\,\mathbf{0}\ \ \mathbf{X}])$ should be block diagonal since this structure is well matched to the spatial covariance of the dual-polarized antenna setup with any antenna spacing (e.g. λ/2 or 4λ)
- $\mathbf{X}$ is a $4 \times N_b$ matrix, where N_b is number of beams ($1 \sim 4$). For each $\mathbf{W}_1$, adjacent overlapping beams are used to reduce the edge effect in the frequency-selective precoding.
- At least sixteen 8Tx DFT vectors are generated from $\mathbf{W}_1$, and a co-phasing via $\mathbf{W}_2$ is performed in order to match with the spatial covariance of the ULA antenna setup and to cope with the phase shift between polarizations.

In Rel. 10, the dual codebook structure is applied only on the 8Tx mode and the 4Tx and 2Tx modes still employ the legacy codebook (Rel. 8 based codebook). According to the recent study in Rel. 11, however, dual codebook scheme is beneficial for 4Tx case such as cross-polarized macro-sites and outdoor small cells with localized antennas [12].

In order to observe the gain of the Rel. 10 dual codebook, we compared performance of Rel. 8 and Rel. 10 codebook. In our simulation, we assume that each UE has a single layer and sends back the feedback information (RI, PMI, and CQI) to the eNB. When the UE is requesting two ranks (2 PMI and 2 CQI), therefore, the eNB regards it as two independent UEs with single layer each. Using all feedback information from the UEs, the eNB performs the MU-MIMO operation. In our simulations, following cases are investigated:

- Extended Rel. 8 codebook (CB): the UE reports a 4-bit PMI. Since the codebook for 8Tx is not defined in LTE Rel. 8, we instead use rank-1 codebook of 802.16m (WiMAX) [13], which is a unitary codebook consisting of 16 elements. Note that Rel. 8 employs wideband PMI only in the MU-MIMO but we also test the subband PMI for the sake of comparison.
- Rel. 10 dual codebook: the UE reports 4-bit wideband PMI $\mathbf{W}_1$ and 4-bit subband PMI $\mathbf{W}_2$ [11].
- Adaptive codebook [14]: In this codebook, $\mathbf{W}_1$ is replaced by the channel covariance matrix $\mathbf{R_t} = \mathbf{E}[\mathbf{H^H H}]$. That is, adaptive codebook consists of the long term channel covariance matrix $\mathbf{R_t}$ and $\mathbf{W}_2$. In order to observe the best possible performance, we used unquantized matrix $\mathbf{R_t}$.

Once the codebook is obtained, we perform the zero-forcing beamforming for each scheme. Let M and K be the number of transmit antennas at the eNB and selected users, respectively, then the transmit signal after the linear precoding becomes $\mathbf{x} = \mathbf{Gu}$ where $\mathbf{G}$ is an $M \times K$ precoding matrix and $\mathbf{u} = (u_1, ..., u_k)^T$ is the user symbol vector. Let $S = \{s_1, ..., s_{|S|}\}$ be the set of users for transmission and $\hat{\mathbf{h}}_k$ is k-th UE's channel response, then the concatenated quantized channel vector becomes $\hat{\mathbf{H}}(S) = [\hat{\mathbf{h}}_{s_1}^T, ..., \hat{\mathbf{h}}_{s_{|S|}}^T]^T$ Note that $\hat{\mathbf{h}}_k$ is k-th UE's channel response given by

$$\hat{\mathbf{h}}_k = \sqrt{\mathbf{L}_k}\mathbf{c}_n^H \tag{2}$$

TABLE III

8×2 ANTENNA CONFIGURATION (XXXX$\rightarrow$ || CHANNELS, 0.5λ ANTENNA SPACING, 8° ANGLE SPREAD)

ZFBF MU-MIMO 8×2 **with MAX 4 LAYERS**	Average cell spectral efficiency (bits/s/Hz)	5% cell edge spectral efficiency (bits/s/Hz)
Extended Rel. 8 codebook (4-bit wideband)	3.26	0.14
Extended Rel. 8 codebook (4-bit subband)	3.30	0.14
Rel. 10 dual codebook ($\mathbf{W}_1$ wideband + $\mathbf{W}_2$ subband)	4.38	0.21
Adaptive codebook (unquantized $\mathbf{R}_t$, report every 500ms)	4.70	0.22

where $\mathbf{c}_n$ is the feedback precoder and $\mathbf{L}_k$ represents UE's large-scale fading. Using $\hat{\mathbf{H}}(S)$, ZF precoding matrix is computed as

$$\mathbf{G}(S) = \mathbf{F}(S)\mathrm{diag}(\mathbf{p})^{1/2} = \mathbf{H}(S)^H(\mathbf{H}(S)\mathbf{H}(S))^{-1}\mathrm{diag}(\mathbf{p})^{1/2} \tag{3}$$

where $\mathbf{f}_k$ is the k-th column of $\mathbf{F}(S)$ and $\mathbf{p} = (p_{s_1}, ..., p_{s_{|S|}})$ is the vector of power normalization coefficients ($p_k = \frac{P}{|S|}\frac{1}{\|\mathbf{f}_k\|^2}$).

Detailed simulation assumptions are provided in Table VI. In real implementation, eNB usually uses cross-polarization considering space limitation for 8Tx. On the orther hand, because it is difficult to implement exact dual polarized antennas in terminal, UE employs single polarization while maximizing antenna spacing within terminal with fixed area. In a nutshell, we simulate XXXX(eNB) $\rightarrow$ ||(UE) configuration, where XXXX and || refer to cross-polarization and single-polarization, respectively. The simulation results are summarized in Table III and Fig. 3. While achieving performance close to the adaptive codebook, Rel. 10 dual codebook achieves 34.3% gain on the average and 50% gain in the cell edge when compared to the extended Rel. 8 codebook. Therefore, we conclude that Rel. 10 dual codebook is very competitive option in cross-polarized antenna setup.

IV. CONCLUDING REMARKS AND FUTURE DIRECTION

In this article, we have reviewed the main features of MU-MIMO techniques adopted in LTE and LTE-A standard. The major enhancement of the downlink MU-MIMO in Rel. 10

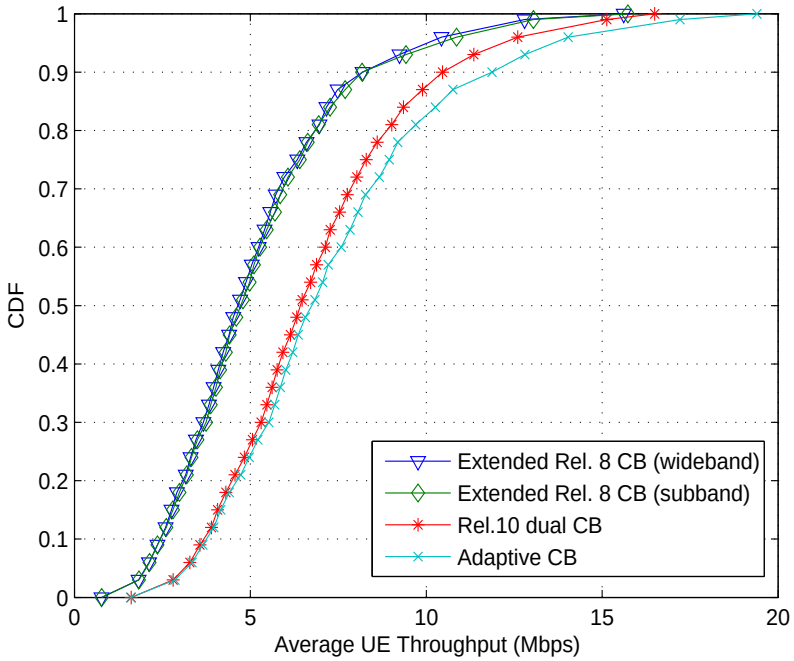

Fig. 3. Average UE throughput for various codebook schemes.

is the support of 8 transmit antennas to allow simultaneous transmission of up to 8 layers. Such enhancement is made possible by the introduction of new measurement and demodulation reference signals enabling non-codebook based precoding and a novel CSI feedback mechanism relying on a high performance and low overhead double codebook structure.

Recently, standardization effort for LTE Rel. 11 has started and the RAN working group is discussing enhancement of downlink MIMO as a study item. Given the importance of the MU-MIMO operation for network operators to meet the increasing user demands of 4G and beyond 4G (B4G) wireless systems, CSI feedback and control signalling will be further improved in future release. Also, future release will pay a particular attention to enhance the MU-MIMO for realistic deployment scenarios. For instance, enhancing the CSI feedback for 4Tx cross-polarized antenna arrays will be one priority. Moreover, given the recent deployment of heterogeneous networks, there is a need in future release to account for small cell deployment when designing the MU-MIMO. MU-MIMO systems will continue to be improved to provide solutions for those issues.

TABLE IV

SYSTEM SIMULATION ASSUMPTIONS

Parameter	**Value**
Duplex method	FDD
Bandwidth	10 MHz
Network synchronization	Synchronized
Cellular Layout	Hexagonal grid, 19 cell sites, 3 sectors per site
Users per sector	10
Downlink transmission scheme	8×2 MU-MIMO ZFBF with rank adaptation with 1 layer per UE
Downlink scheduler	Proportional Fair scheduling in the frequency and time domain.
Downlink link adaptation	CQI and PMI 5ms feedback period 1 PMI and 1 CQI feedback per subband (=4 consecutive RBs) 6ms delay total (measurement in subframe n is used in subframe n+6) Unquantized CQI, PMI feedback error: 0% MCSs based on LTE transport formats [36.213]
Allocation	localized
Downlink HARQ	Maximum 3 re-transmissions, IR, no error on ACK/NACK, 8 ms delay between re-transmissions
Downlink receiver type	MMSE based on DM RS of serving cell
Channel estimation	Non-ideal channel estimation on CSI-RS and DM-RS vs. CINR curves based on LLS provided as an input to SLS.
Antenna configuration	$\mathrm{XXXX}->\|\|$ channels, 0.5λ antenna spacing, 8° angle spread
Control Channel overhead, Acknowledgements etc.	LTE: L=3 symbols for DL CCHs Overhead of DM-RS: RANK 1, 2 : 12 REs/RB/subframe Overhead of CSI-RS: 4/8 sets of CSI-RS every 5 ms and 1RE/port/RB (This is, in 8Tx antenna case, 8 REs/RB per 5ms) Overhead of 2-ports CRS
BS antenna downtilt	Case 1 3GPP 3D: 15 deg
Channel model	SCM urban macro high/low spread for 3GPP case 1, 3km/h
Intercell interference modeling	7 intercell interference links are explicitly considered. The remaining links are modeled with Rayleigh distribution.
Max. number of layers (UEs)	4

REFERENCES

[1] http://network4g.verizonwireless.com/#/4g-network-verizon-wireless

[2] Erik Dahlman, Stefan Parkvall, and Johan Skold, 4G LTE/LTE-Advanced for Mobile Broadband. Academic Press, 2011.

[3] F. Boccardi, B. Clerckx, A. Ghosh, E. Hardouin, G. Jongren, K. Kusume, E. Onggosanusi, Y. Tang, "Multiple-Antenna Techniques in LTE-Advanced," *IIEEE Comm. Mag.*, vol. 50, no. 3, Mar. 2012, pp. 114-121.

[4] T. Yoo, N. Jindal, A. Goldsmith, "Finite-rate feedback MIMO broadcast channels with a large number of users," in Proc. of IEEE ISIT, pp. 1214-1218, July. 2006.

[5] 3GPP TS 36.913, "Evolved Universal Terrestrial Radio Access (E-UTRA); Requirements for further advancements for Evolved Universal Terrestrial Radio Access (E-UTRA) LTE-Advanced".

[6] M. Sharif and B. Hassibi, "On the capacity of MIMO broadcast channels with partial side infonnation," *IEEE Trans. Inf. Theory*, vol. 51, no. 2, Feb. 2005, pp. 506-522.

[7] T. Yoo, A. Goldsmith, "On the optimality of multiantenna broadcast scheduling using Zero-forcing beamforming," *IEEE J. Select. Areas Commun.*, vol. 24, no. 3, March 2006, pp. 528-541.

[8] 3GPP TSG RAN WG1 #60, R1-101129, "On Extensions to Rel-8 PMI Feedback," February 2010.

[9] 3GPP TSG RAN WG1 #61, R1-103332, "Way Forward on UE Feedback," May 2010.

[10] 3GPP TSG RAN WG1 #61, R1-103378, "Performance evaluations of Rel.10 feedback framework," May, 2010.

[11] 3GPP TSG RAN WG1 #62, R1-105011, "Way Forward on 8Tx Codebook for Rel.10 DL MIMO," August 2010.

[12] 3GPP TR 36.871 V11.0.0, "Evolved Universal Terrestrial Radio Access (E-UTRA); Downlink Multiple Input Multiple Output (MIMO) enhancement for LTE-Advanced (Release 11)".

[13] IEEE Std 802.16m^{TM}-2011, "Amendant3: Advanced Air Interface," May, 2011, pp. 740.

[14] 3GPP TSG RAN WG1 #58, R1-093059, "Adaptive Feedback: A New Perspective of the Adaptive Codebook," August 2009.

PLACE
PHOTO
HERE

Chaiman Lim is currently working toward the Ph.D. degree School of Information and Communication, Korea University, Seoul, Korea. His research interests include communications and information theory, signal processing for wireless communications, and advanced MIMO systems.

PLACE
PHOTO
HERE

Taesang Yoo received the B.S. degree (Hons.) in Electrical Engineering from Seoul National University, Seoul, Korea, in 1998, and the M.S. and Ph.D. degrees in Electrical Engineering from Stanford University, Stanford, CA, in 2003 and 2007. Since 2006, he has been with Corporate Research and Development of Qualcomm, where he is currently working on 3GPP Long Term Evolution (LTE) and LTE-Advanced wireless systems. His research interests include heterogeneous cellular networks, multiple antenna systems, receiver algorithms, and various design and performance aspects of LTE/LTE-A systems and standards.

PLACE
PHOTO
HERE

Bruno Clerckx received the Ph.D. degree from Universite catholique de Louvain, Belgium. He held visiting research positions at Stanford University and EURECOM and was with Samsung Electronics from 2006 to 2011. He actively contributed to 3GPP LTE/LTE-A and acted as the rapporteur for the 3GPP CoMP Study Item. He is now a Lecturer (Assistant Professor) at Imperial College London and an editor for IEEE Transactions on Communications.

PLACE
PHOTO
HERE

Byungju Lee received the B.S. degree in the School of Information and Communication, Korea University, Seoul, Korea, in 2008, where he is currently working toward the Ph.D. degree. His research interests include wireless communications and network information theory.

PLACE
PHOTO
HERE

Byonghyo Shim received the B.S. and M.S. degrees in control and instrumentation engineering from Seoul National University, Korea, in 1995 and 1997, respectively, and the M.S. degree in mathematics and the Ph.D. degree in electrical and computer engineering from the University of Illinois at Urbana-Champaign, in 2004 and 2005, respectively. From 2005 to 2007, he worked for Qualcomm Incorporated. Since September 2007, he has been with the school of information and communication, Korea University, where he is currently an associate professor.